

Tunable lower critical fractal dimension for a non-equilibrium phase transition

Mattheus Burkhard, Luca Giacomelli, and Cristiano Ciuti

Université Paris Cité, CNRS, Matériaux et Phénomènes Quantiques, 75013 Paris, France

(Dated: June 26, 2025)

We theoretically investigate the role of spatial dimension and driving frequency in a non-equilibrium phase transition of a driven-dissipative interacting bosonic system. In this setting, spatial dimension is dictated by the shape of the external driving field. We consider both homogeneous driving configurations, which correspond to standard integer-dimensional systems, and fractal driving patterns, which give rise to a non-integer Hausdorff dimension for the spatial density. The onset of criticality is characterized by critical slowing down in the excited density dynamics as the system asymptotically approaches the steady state, signaling the closing of the Liouvillian frequency gap. We show that the lower critical dimension —below which the non-equilibrium phase transition ceases to occur— can be controlled continuously by the frequency detuning of the driving field.

Introduction — A phase transition [1] for a physical system manifests as a discontinuous behavior of observable quantities emerging in some thermodynamic limit. In this context, the spatial dimension plays a key role in determining critical behavior. A particularly important concept in this regard is the lower critical dimension d_L : a phase transition that occurs for dimension $d \geq d_L$ ceases to exist for $d < d_L$, as fluctuations in lower-dimensional systems tend to suppress singularities.

Non-equilibrium [2] phase transitions are critical phenomena that remain less explored and understood compared to their equilibrium counterparts. A critical point of a non-equilibrium system can be characterized by a critical slowing down of the system dynamics approaching the steady-state in a thermodynamical limit [3]. In the Liouvillian framework, this is equivalent to studying the closing of the frequency gap associated to the master equation describing the non-equilibrium dynamics of the density matrix [3]. Interacting optical systems [4] are particularly well-suited for studying such transitions due to the precise control of external driving, nonlinearities and the accurate characterization of losses, which compete in shaping non-trivial non-equilibrium dynamics and steady-state [5–14]. For interacting bosons such as photons, in addition to the usual thermodynamic limit of large spatial size, critical behavior emerges in another thermodynamic limit when the physical parameters are tuned in such a way that the number of bosons in the state becomes arbitrarily large. This has been shown to occur both theoretically and experimentally in driven systems consisting of a single two-level atom coupled to single cavity photon mode [6, 8] or a driven single cavity mode with Kerr nonlinearity [15–17], achieved in the limit of weak photon nonlinearity. Here, we will focus primarily on the conventional thermodynamic limit of large spatial size, which, in the context of optics, corresponds to an infinite number of modes.

While the role of integer spatial dimensions in equilibrium critical phenomena is well studied, the influence of non-integer dimensions, particularly in fractal patterns, is not as much understood even in equilibrium sys-

tems [18–21]. Notably, studies on the equilibrium Ising model [22] suggested that the critical behavior is not solely determined by the fractal (Hausdorff) dimension but also other geometrical attributes [22–25].

Recent studies on driven-dissipative interacting bosonic systems have revealed critical behavior in the limit of large spatial size, particularly in two-dimensional (2D) systems [26–28]. In these systems, a first-order phase transition manifests as a discontinuous jump in the bosonic density at a critical driving intensity. A theoretical study demonstrated that, within a range of frequency detunings close to the dissipation rate, these systems exhibit an emergent equilibrium behavior that can be mapped onto the equilibrium Ising model [26]. In this analogy, the high- and low-density phases correspond to the two states of the Ising variable. Since the Ising model is known to undergo a phase transition in 2D but not in 1D, a similar dimensional dependence is expected for these driven-dissipative systems. A subsequent study on continuous systems, where the effective dimension is imprinted by a properly shaped optical driving field [28], confirmed this behavior: a phase transition emerges in 2D but remains absent in 1D when the frequency detuning is close to the linear-regime dissipation rate. However, the role of frequency detuning was not explored further. Additionally it remained unclear what behavior would characterize the system at intermediate dimensions, that in continuous systems can be naturally obtained by shaping the driving field. Indeed, the impact of fluctuations due to many-mode dynamics strongly depends on the spatial dimension.

Several fundamental questions have never been considered: What happens to this class of non-equilibrium phase transitions in fractional dimensions? Does the system exhibit a lower critical dimension below which no phase transition occurs? How does frequency detuning influence this critical dimension? Addressing these fundamental questions is central to the present work, as they may unveil new paradigms in non-equilibrium critical behavior.

In this Letter, we investigate the phase transition

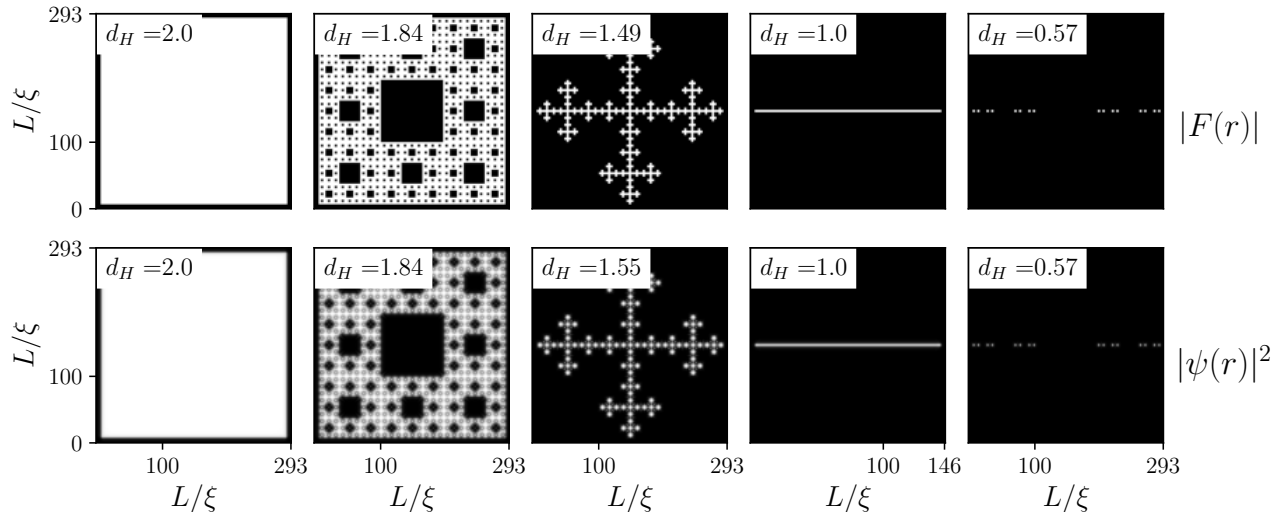


FIG. 1. Driving intensity patterns (top panels) and grayscale maps (bottom panels) of the corresponding steady-state bosonic densities. Each column shows the spatial profile of a fractal pattern along with its associated Hausdorff box-counting dimension d_H . The first (fourth) column shows a 2D (1D) pattern with an integer dimension. The second (third) column displays results for a Sierpinski carpet (cross) after three iterations. The last column shows a system with dimension lower than one, a Cantor set with three iterations, corresponding to a system size with side length $L = 3^4 l$, where l is defined in the text. All figures obtained with the pump frequency detuning $\Delta = \gamma$ and with the driving amplitudes tuned to their respective critical points.

of a driven-dissipative, continuous, and interacting 2D bosonic gas. We use both homogeneous and fractal-shaped driving patterns to impose different Hausdorff dimensions. We demonstrate that critical behavior is strikingly governed by both the Hausdorff dimension and the frequency detuning of the driving.

Theoretical framework — We consider a system of interacting bosons whose driven-dissipative dynamics can be described by a two-dimensional non-equilibrium Gross-Pitaevskii equation [4, 28, 29], namely:

$$i \frac{d\psi}{dt} = \left[-\Delta - \frac{\hbar \nabla^2}{2m} + g |\psi|^2 - i \frac{\gamma}{2} \right] \psi + i F(\mathbf{r}). \quad (1)$$

Here, $\psi(\mathbf{r}, t)$ denotes the mean value of the bosonic field operator, depending on the two-dimensional spatial position \mathbf{r} and time t . The equation is in the so-called pump rotating frame, where the frequency detuning Δ represents the difference between the driving frequency and the frequency of the boson mode with zero wavevector (corresponding to the lowest frequency mode). The non-linear repulsive interaction is quantified by g , while γ characterizes the natural dissipation rate of the system. In the following, we will express lengths in units of the characteristic length $\xi = \sqrt{\frac{\hbar}{2m\gamma}}$. Finally, $F(\mathbf{r})$ denotes the spatially dependent driving field.

In this class of systems, a phase transition manifests in a sharp increase of the bosonic density $n = |\psi|^2$ when the driving intensity $I = |F|^2$ reaches a critical value I_c [26–28]. This is related to the bistable behaviour in the mean-field treatment for detunings $\Delta > \sqrt{3}/2 \gamma$ [4, 15], whose

robustness to fluctuations depends on dimension. Above the critical dimension, a sharp jump of the density is obtained in the thermodynamic limit of an infinite system size. This corresponds to a first-order phase transition from a dark (low boson density) to a bright (high boson density) state.

The effective spatial dimension can be controlled with the spatial shape of the driving field $F(\mathbf{r})$: pumping uniformly over a region of the plane results in a two-dimensional system with diffusive boundary conditions (see first column of Fig. 1), while imposing a different geometry results in a lower dimension. For example, a pump profile that is narrow in one direction and elongated in the other creates an effectively one-dimensional system [28] (fourth column of Fig. 1). But this can be extended to non-integer dimensions if the driving field has a fractal shape, as exemplified in the second and third columns of Fig. 1, where a Sierpinski carpet and a Sierpinski cross with a finite number of iterations are shown.

Note that the resulting bosonic density has in general a slightly distorted shape, as shown in the lower panels of Fig. 1 (more patterns are shown in the Supplementary Material [30]). For example, in the second column, smaller holes in the Sierpinski carpet are partially filled and more affected than larger holes. This is due mainly to interference and dispersive effects, as well as the non-linear boson-boson interactions, that introduce intrinsic length scales in the system. Despite these distortions and the finite size, the resulting patterns possess their own fractal dimension (slightly different from the nominal one of the ideal, infinitely self-similar patterns) that

can be quantified with the box-counting method [30, 31] (for more details see [32]). In Fig. 1, we have annotated both the pump pattern and the resulting densities with their respective box-counting dimensions d_H . Importantly, even in the presence of distortions and finite-size effects, the extracted dimensions remain fractional and close to the nominal one.

While for integer-dimensional configuration the system size can be changed continuously, reaching the thermodynamic limit of a fractal system is less straightforward and can be approached in several ways. Here, we consider the limit obtained by increasing the total system size while keeping the length of the smallest structural detail l constant, as illustrated in Fig. 2(a). In all calculations reported in this work, we take $l = 3.45\xi$. If this length were allowed to vary, the smallest elements of the pattern would change with system size, thereby changing its ratio to the intrinsic physical length scales and drastically altering its box counting dimension. Moreover, to maintain the fractal structure as the system grows, at each step we also increase the number of self-similar iterations. For example for the Sierpinski carpet, this implies that the linear size triples with each additional iteration, as depicted in Fig. 2(a). Although this exponential growth poses computational challenges, we were able to reach sufficiently large system sizes to observe the emergence of the asymptotic behavior characteristic of the thermodynamic limit.

Phase transition markers — In the investigation of phase transitions, several markers serve as key indicators for identifying their presence or absence. One such marker is the maximal slope of the spatially averaged steady-state density as a function of the input intensity. In particular, when a first-order phase transition occurs, this slope diverges, signaling a discontinuous change in the system's behavior [28]. Another crucial indicator is the asymptotic decay rate λ , also referred to as the Liouvillian gap in the Lindbladian framework [3, 5]. At long times, the system relaxes exponentially towards its steady state with a decay rate λ , whose inverse is the characteristic timescale for equilibration. At the critical point of a driven-dissipative phase transition, $I = I_c$, one expects critical slowing down, namely the system requires an infinite amount of time to reach its steady state. In other words, at critical driving the asymptotic decay rate λ tends to zero in the thermodynamic limit [3, 15]. Conversely, if in this infinite-size limit the decay rate remains finite for all values of the driving intensity, no phase transition occurs.

The asymptotic decay rate λ can be obtained from the time-dependence of the spatially averaged density $\bar{n}(t) = \int d^2x n(t, x)$, that at long times will evolve as $\bar{n}(t) - \bar{n}_{ss} \propto e^{-\lambda t}$, where \bar{n}_{ss} is its steady-state value. We compute this value by numerically evolving the dynamical equation (1) and performing a Fourier analysis of $\bar{n}(t)$. This procedure is repeated for different driving intensi-

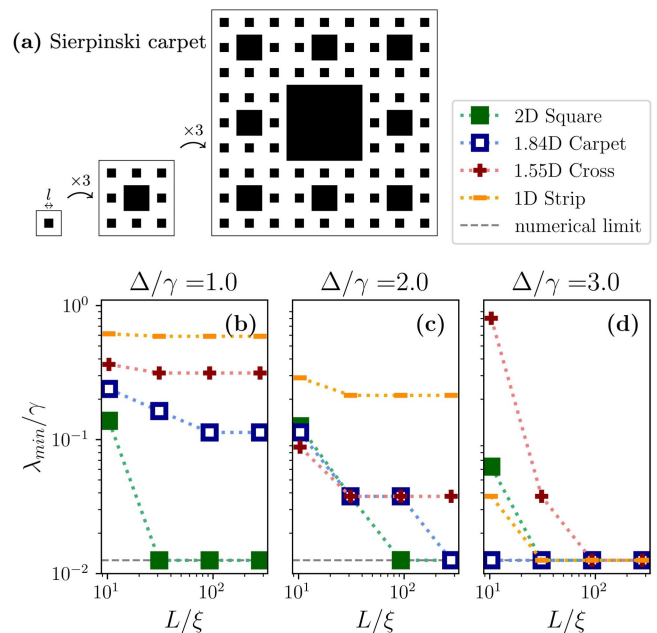


FIG. 2. (a) Illustration of the approach to the thermodynamic limit by expanding the size of a fractal pattern. At each step, the total linear size L is multiplied by three, while the smallest resolved feature l remains constant. (b–d): Minimal asymptotic decay rate λ_{\min} as a function of the linear system size L for detuning values $\Delta = 1.0\gamma$, $\Delta = 2.0\gamma$, and $\Delta = 3.0\gamma$. Different markers correspond to different spatial geometries indicated in the legend.

ties I , to find the smallest value of λ , i.e. the minimal asymptotic decay rate $\lambda_{\min} = \min_I \lambda(I)$. To probe the presence of a critical behaviour, we compare the values of λ_{\min} obtained for different system sizes: a critical point is present if this quantity tends to zero for increasing system sizes, while it is absent if it saturates to a finite value.

Results at fixed detuning — We begin by examining the well-studied detuning $\Delta = \gamma$, for which in previous investigations the first-order phase transition was found to occur in a two-dimensional system, and to be absent in a one-dimensional one [26–28]. This is confirmed by our calculations of λ_{\min} , whose dependence on the system size is shown in Fig. 2(b), with green squares for a 2D system and orange bars for a 1D system. Here and later, for each geometry we computed λ_{\min} for a range of driving intensities and identified the minimal value. In fact, for the 2D case and in the limit of large systems, λ_{\min} vanishes (with a precision given by the numerical resolution, which is set by the final time of the calculated temporal dynamics). For the considered detuning, this critical slowing down is instead absent in the one-dimensional system, as λ_{\min} saturates to a finite value.

We extended this investigation to fractal dimensions. For example, for the Sierpinski carpet (second column of Fig. 1), λ_{\min} has a minimum around the expected mean-

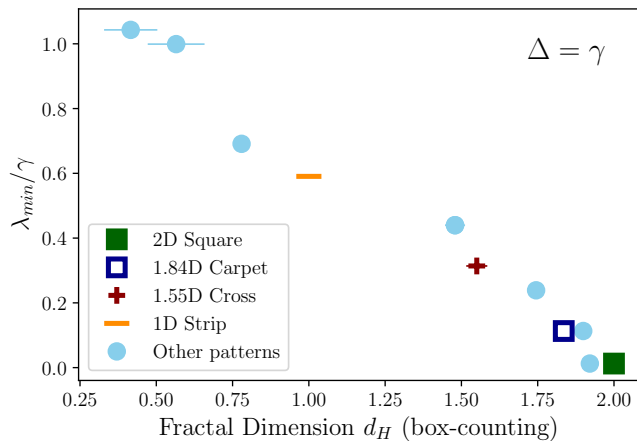


FIG. 3. Minimal asymptotic decay rate λ_{\min} versus Hausdorff dimension for a fixed detuning $\Delta = \gamma$. The driving patterns associated with the various points are visualized in the Supplementary Material. Horizontal error bars show the uncertainty of the box-counting method. System sizes are reported in the main text.

field critical driving [30], but the value of this minimum converges to a finite value for increasing system size, as shown in Fig. 2(b) with empty blue square markers. The system therefore exhibits slowing down, but it is not critical. The shape of this slowest mode is non-trivial and will be the object of further studies [30]. However we can say that, for this value of the detuning, the Sierpinski carpet of dimension $d_H \simeq 1.84$ is below the critical dimension. This can be also characterized in terms of the steady-state average density, that does not display a discontinuous jump as a function of I , and has instead a smooth crossover from the low density to the high density phase [30]. We obtain a similar behavior for the Sierpinski cross (third column of Fig. 1), which has $d_H \simeq 1.5$ and whose convergence of λ_{\min} to a finite value is shown with red cross markers in Fig. 2(b).

The actual value of λ_{\min} also quantifies how far the system is from criticality, and we found it to depend strongly on the system's dimensionality. This is shown in Fig. 3, where we report the minimal asymptotic decay rate as a function of the Hausdorff dimension d_H , for a variety of fractal geometries (the patterns for the light blue circular markers are shown in [30]). These values are the ones for the largest computationally feasible sizes (ranging from $L = 81l$ to $L = 216l$, depending on the geometry), that are representative of the thermodynamical limit $\lim_{L \rightarrow \infty} \lambda_{\min}$, since we assured convergence of this value. The difference between λ_{\min} for the two largest considered sizes gives us a vertical error bar that is always smaller than the marker size. The horizontal error bars are instead the moderate uncertainty in the Hausdorff dimension given by the box-counting method, which is more significant for patterns that have a fractal di-

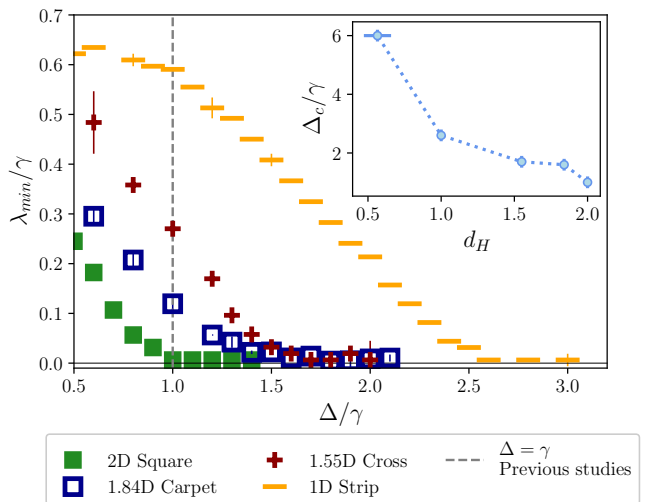


FIG. 4. Minimal asymptotic decay rate as a function of detuning Δ for different spatial dimensions. All data points are obtained for a system size $L = 81l$. The vertical error bars represent the difference in λ_{\min} between this size and $L = 27l$, providing an estimate of the finite-size effects and our proximity to the thermodynamic limit. Inset: Critical detuning Δ_c as a function of the Hausdorff dimension d_H . Error bars correspond to the numerical resolution of our simulation.

mension smaller than one (Cantor sets). Remarkably, we have found that λ_{\min} exhibits a clear monotonous dependence on the Hausdorff dimension d_H , with the slowing down continuously approaching a critical one while the dimension is increased. In this case $\Delta = \gamma$, we observe that the decay rate only tends to zero when the dimension tends to two, i.e. the lower critical dimension for the first-order phase transition is $d_L(\Delta = \gamma) = 2$. This extends previous results [26–28] to fractional dimensions, but, as we will show in the following, we have made the remarkable discovery that the lower critical dimension surprisingly decreases significantly from 2 as the detuning Δ increases.

Changing the lower critical dimension — As shown in Figs. 2(c)-(d) and in Fig. 4, increasing the driving detuning Δ leads to a systematic decrease of λ_{\min} , and eventually to its vanishing, for all geometries. This implies that the system is critical and exhibits a first-order phase transition even for dimensions $d_H < 2$, provided that the ratio Δ/γ is large enough. We define the critical detuning Δ_c as the value above which λ_{\min} vanishes in the thermodynamical limit. This value is geometry-dependent: for the 2D system (green squares), it is $\Delta_c \simeq 1.0\gamma$, close to the known previously studied case. The critical detuning Δ_c is larger for lower-dimensional systems. This can be seen in Fig. 2(c), where, for large enough systems, λ_{\min} vanishes not only for the 2D square, but also for the Sierpinski carpet, which for $\Delta = \gamma$ is not critical. Correspondingly, the smooth crossover in the average density for $\Delta = \gamma$, becomes a sharp discontinuity

[30]. For $\Delta = 2\gamma$ the lower-dimensional Sierpinski cross and the one-dimensional system are still non-critical, but both become for a higher $\Delta = 3\gamma$, as shown in Fig. 2(d). These results show that it is possible to tune the lower critical dimension, or, in other words, to make the phase transition occur at any fixed dimension by increasing Δ . The inset of Fig. 4, shows that the lower critical dimension decreases continuously as the Hausdorff dimension is changed. Interestingly, also the 1D case and fractals with dimension lower than one (e.g., Cantor sets) can be made critical by increasing Δ/γ enough. In fact, in the limit $d_H \rightarrow 0^+$, we can expect $\Delta_c \rightarrow +\infty$. Indeed, for a zero-dimensional (one-mode) nonlinear bosonic resonator, it is known that the asymptotic decay rate vanishes only in the limit of infinite detuning [16, 33].

Conclusions — In conclusion, we have demonstrated that in driven-dissipative systems of interacting bosons, the lower critical dimension can be continuously tuned with the frequency detuning of the driving field and can be fractional. This establishes a novel paradigm in the study of non-equilibrium phase transitions, where geometry and external drive jointly control critical behavior.

Our results were obtained by solving the many-mode mean-field dynamics and analyzing the emergence of critical slowing down as the size of the driving patterns increases. An open and important question concerns the fate of the lower critical dimension in the presence of strong quantum boson-boson interactions, beyond the many-mode mean-field regime, particularly in the hardcore boson limit. Three scenarios could take place: (i) the lower critical dimension is the same in the strongly correlated regime; (ii) the lower critical dimension could evolve continuously with interaction strength, or (iii) a discontinuous shift could occur, signaling the emergence of a quantum phase transition with new phases in the strongly quantum correlated regime. Exploring this limit remains a key direction for future research. Another promising avenue is to investigate how fractional dimension and driven-dissipative conditions influence other classes of non-equilibrium phase transitions. This could yield deeper insight into the fundamental role of spatial geometry and dissipation in shaping critical phenomena in classical and quantum open systems.

We acknowledge support from the French ANR project FracTrans (grant ANR-24-CE30-6983) and a grant (Polaritonic) from the French Government managed by the ANR under the France 2030 programme with the reference ANR-24-RR11-0001. This work was also funded by the French ministry of research through a CDSN grant of ENS Paris-Saclay.

- [2] H.-P. Breuer, F. Petruccione, H.-P. Breuer, and F. Petruccione, *The Theory of Open Quantum Systems* (Oxford University Press, Oxford, New York, 2002).
- [3] F. Minganti, A. Biella, N. Bartolo, and C. Ciuti, Spectral theory of Liouvillians for dissipative phase transitions, *Phys. Rev. A* **98**, 042118 (2018).
- [4] I. Carusotto and C. Ciuti, Quantum fluids of light, *Rev. Mod. Phys.* **85**, 299 (2013).
- [5] E. M. Kessler, G. Giedke, A. Imamoglu, S. F. Yelin, M. D. Lukin, and J. I. Cirac, Dissipative phase transition in a central spin system, *Phys. Rev. A* **86**, 012116 (2012).
- [6] H. Carmichael, Breakdown of Photon Blockade: A Dissipative Quantum Phase Transition in Zero Dimensions, *Physical Review X* **5**, 031028 (2015).
- [7] N. Bartolo, F. Minganti, W. Casteels, and C. Ciuti, Exact steady state of a Kerr resonator with one- and two-photon driving and dissipation: Controllable Wigner-function multimodality and dissipative phase transitions, *Physical Review A* **94**, 033841 (2016).
- [8] J. M. Fink, A. Dombi, A. Vukics, A. Wallraff, and P. Domokos, Observation of the photon-blockade breakdown phase transition, *Phys. Rev. X* **7**, 011012 (2017).
- [9] A. Biella, F. Storme, J. Lebreuilly, D. Rossini, R. Fazio, I. Carusotto, and C. Ciuti, Phase diagram of incoherently driven strongly correlated photonic lattices, *Physical Review A* **96**, 023839 (2017).
- [10] M. Biondi, G. Blatter, H. E. Türeci, and S. Schmidt, Nonequilibrium gas-liquid transition in the driven-dissipative photonic lattice, *Physical Review A* **96**, 043809 (2017).
- [11] M. Fitzpatrick, N. M. Sundaresan, A. C. Y. Li, J. Koch, and A. A. Houck, Observation of a dissipative phase transition in a one-dimensional circuit qed lattice, *Phys. Rev. X* **7**, 011016 (2017).
- [12] A. Vukics, A. Dombi, J. M. Fink, and P. Domokos, Finite-size scaling of the photon-blockade breakdown dissipative quantum phase transition, *Quantum* **3**, 150 (2019).
- [13] R. Sett, F. Hassani, D. Phan, S. Barzanjeh, A. Vukics, and J. M. Fink, Emergent macroscopic bistability induced by a single superconducting qubit, *PRX Quantum* **5**, 010327 (2024).
- [14] M. Yao, A. Lingenfelter, R. Belyansky, D. Roberts, and A. A. Clerk, Hidden time reversal in driven xzx spin chains: Exact solutions and new dissipative phase transitions, *Phys. Rev. Lett.* **134**, 130404 (2025).
- [15] W. Casteels, R. Fazio, and C. Ciuti, Critical dynamical properties of a first-order dissipative phase transition, *Phys. Rev. A* **95**, 012128 (2017).
- [16] S. R. K. Rodriguez, W. Casteels, F. Storme, N. Carlon Zambon, I. Sagnes, L. Le Gratiet, E. Galopin, A. Lemaître, A. Amo, C. Ciuti, and J. Bloch, Probing a dissipative phase transition via dynamical optical hysteresis, *Phys. Rev. Lett.* **118**, 247402 (2017).
- [17] T. Fink, A. Schade, S. Höfling, C. Schneider, and A. Imamoglu, Signatures of a dissipative phase transition in photon correlation measurements, *Nature Physics* **14**, 365–369 (2017).
- [18] B. B. Mandelbrot, *The Fractal Geometry of Nature* (Henry Holt and Company, 1983) google-Books-ID: SWc-PAQAAMAAJ.
- [19] J. Genzor, A. Gendiar, and T. Nishino, Phase transition of the Ising model on a fractal lattice, *Phys. Rev. E* **93**, 012141 (2016).

[1] S.-K. Ma, *Modern Theory of Critical Phenomena*, 1st ed. (Routledge, New York, 2001) p. 591.

- [20] Z. Zhou, X.-F. Zhang, F. Pollmann, and Y. You, [Fractal Quantum Phase Transitions: Critical Phenomena Beyond Renormalization](#) (2021).
- [21] N. E. Myerson-Jain, S. Yan, D. Weld, and C. Xu, Construction of Fractal Order and Phase Transition with Rydberg Atoms, [Physical Review Letters](#) **128**, 017601 (2022).
- [22] Y. Gefen, B. B. Mandelbrot, and A. Aharony, Critical phenomena on fractal lattices, [Phys. Rev. Lett.](#) **45**, 855 (1980).
- [23] J. M. Carmona, U. M. B. Marconi, J. J. Ruiz-Lorenzo, and A. Tarancón, Critical properties of the Ising model on Sierpinski fractals: A finite-size scaling-analysis approach, [Phys. Rev. B](#) **58**, 14387 (1998).
- [24] M. Perreau, Ising model in planar lacunary and fractal lattices: A path counting approach, [Phys. Rev. B](#) **96**, 174407 (2017).
- [25] H. Yi, Quantum critical behavior of the quantum Ising model on fractal lattices, [Phys. Rev. E](#) **91**, 012118 (2015).
- [26] M. Foss-Feig, P. Niroula, J. T. Young, M. Hafezi, A. V. Gorshkov, R. M. Wilson, and M. F. Maghrebi, Emergent equilibrium in many-body optical bistability, [Phys. Rev. A](#) **95**, 043826 (2017).
- [27] F. Vicentini, F. Minganti, R. Rota, G. Orso, and C. Ciuti, Critical slowing down in driven-dissipative Bose-Hubbard lattices, [Phys. Rev. A](#) **97**, 013853 (2018).
- [28] Z. Li, F. Claude, T. Boulier, E. Giacobino, Q. Glorieux, A. Bramati, and C. Ciuti, Dissipative phase transition with driving-controlled spatial dimension and diffusive boundary conditions, [Phys. Rev. Lett.](#) **128**, 093601 (2022).
- [29] A. Le Boité, G. Orso, and C. Ciuti, Bose-Hubbard model: Relation between driven-dissipative steady states and equilibrium quantum phases, [Phys. Rev. A](#) **90**, 063821 (2014).
- [30] See Supplemental Material at URL-will-be-inserted-by-publisher.
- [31] J. Theiler, Estimating fractal dimension, [J. Opt. Soc. Am. A](#) **7**, 1055 (1990).
- [32] This method quantifies the fractal dimension by overlaying a grid of s^2 square boxes, each of edge length L/s , where L is the system size. After applying a thresholding algorithm [34] to extract the structure from a grayscale image, the number of boxes A that intersect the pattern is counted. Assuming a scaling relation $A \sim s^{d_H}$, the fractal (Hausdorff) dimension d_H is obtained as the slope of $\log A$ versus $\log s$ over a range of scales. More details are provided in the Supplementary Materials [30].
- [33] W. Casteels, F. Storme, A. Le Boité, and C. Ciuti, Power laws in the dynamic hysteresis of quantum nonlinear photonic resonators, [Phys. Rev. A](#) **93**, 033824 (2016).
- [34] N. Otsu, A threshold selection method from gray-level histograms, [IEEE Transactions on Systems, Man, and Cybernetics](#) **9**, 62 (1979).

Supplementary Material for the article: “Tunable lower critical fractal dimension for a non-equilibrium phase transition”

Mattheus Burkhard, Luca Giacomelli, and Cristiano Ciuti
Université Paris Cité, CNRS, Matériaux et Phénomènes Quantiques, 75013 Paris, France

(Dated: June 26, 2025)

This Supplementary Material provides further theoretical details and additional numerical results that support and extend the findings presented in the main text.

THE EFFECT OF DETUNING FOR A SIERPINSKI CARPET

In the main text, we characterize critical behavior in terms of the minimal asymptotic decay rate. Here, we further examine how the asymptotic decay rate depends on the driving intensity for different system sizes. In Fig. S.1(a)–(b), these quantities are shown for the Sierpinski carpet (first row in Fig. 1) with $\Delta = \gamma$, a regime where no phase transition occurs. The minimal asymptotic decay rate exhibits a clear minimum around a critical driving intensity $I \approx 2.2\gamma^2$, yet this minimum saturates to a finite value. Correspondingly, the density increases smoothly across all system sizes, deviating from the homogeneous single-mode mean-field prediction [4] (dashed grey curve) obtained by retaining only the homogeneous $k = 0$ mode.

In Fig. S.1(c)–(d), we plot the same quantities for a larger detuning, $\Delta = 2\gamma$. In this case, at a higher driving intensity $I_c \approx 7.1\gamma^2$, the minimal asymptotic decay rate λ_{\min} collapses to numerical precision, and the density exhibits an abrupt switch from the lower to the upper branch of the bistability. These features indicate the occurrence of a first-order phase transition.

BOX-COUNTING DIMENSION

To quantify the fractal dimension of the considered patterns, we employed the box-counting method [31]. The shape of each pattern is first extracted from a grayscale image (see, for example, Fig. 1) by applying a threshold above which points are considered part of the pattern [34]. This thresholding procedure delineates the fractal structure within the image, effectively separating the foreground (pattern) from the background and yielding a binary representation. In this binary image, pixels above the threshold are marked as belonging to the pattern, while those below are discarded. This representation serves as the basis for further spatial analysis.

The box-counting method then divides the binary image into a grid of s^2 square boxes, each with edge length $b = L/s$, where L is the linear size of the system. We count the number of boxes that intersect the pattern, thereby estimating the area A of the fractal (in units of b^2). In principle, this area scales as $A \propto s^{d_H}$, where d_H is the Hausdorff (fractal) dimension. The box-counting dimension is thus given by the slope of $\log A = f(\log s)$ obtained over different scales s . By performing a linear fit to this curve, we extract an estimate of d_H , and the corresponding uncertainty is reported in the main text as the error bar on the box-counting dimension.

The patterns in Fig. 1 are annotated with their respective box-counting dimensions d_H , which differ slightly from the theoretical values d_H^{th} for *perfect*, infinitely self-similar fractals. For example, for the Sierpinski carpet (second column), $d_H^{th} = 1.89$, and for the Sierpinski cross (third column), $d_H^{th} = 1.46$. Nevertheless, even for these distorted and finite structures, we can determine a fractal dimension lying between 1 and 2.

For patterns with fractal dimension equal to or lower than 1 (Fig. 1, last column), we used a slightly modified version of the box-counting method. We restricted the analysis to the horizontal dimension by fixing the vertical box size to the system size L , while the horizontal box length still scales as $b = L/s$. Instead of square boxes of size b^2 , we thus used rectangular boxes of size bL . This allows for a consistent evaluation of fractal dimensions ranging from 0 to 2.

For integer-dimensional patterns (1D and 2D), we did not apply the box-counting method, as their Hausdorff dimensions are trivially $d_H = 1$ and $d_H = 2$, respectively. Nonetheless, one could apply box-counting to the patterns shown in the first and fourth columns of Fig. 1; such an analysis would yield values close to 1 or 2, but never exactly. Indeed, precisely capturing integer dimensions via box-counting is challenging due to inherent estimation errors.

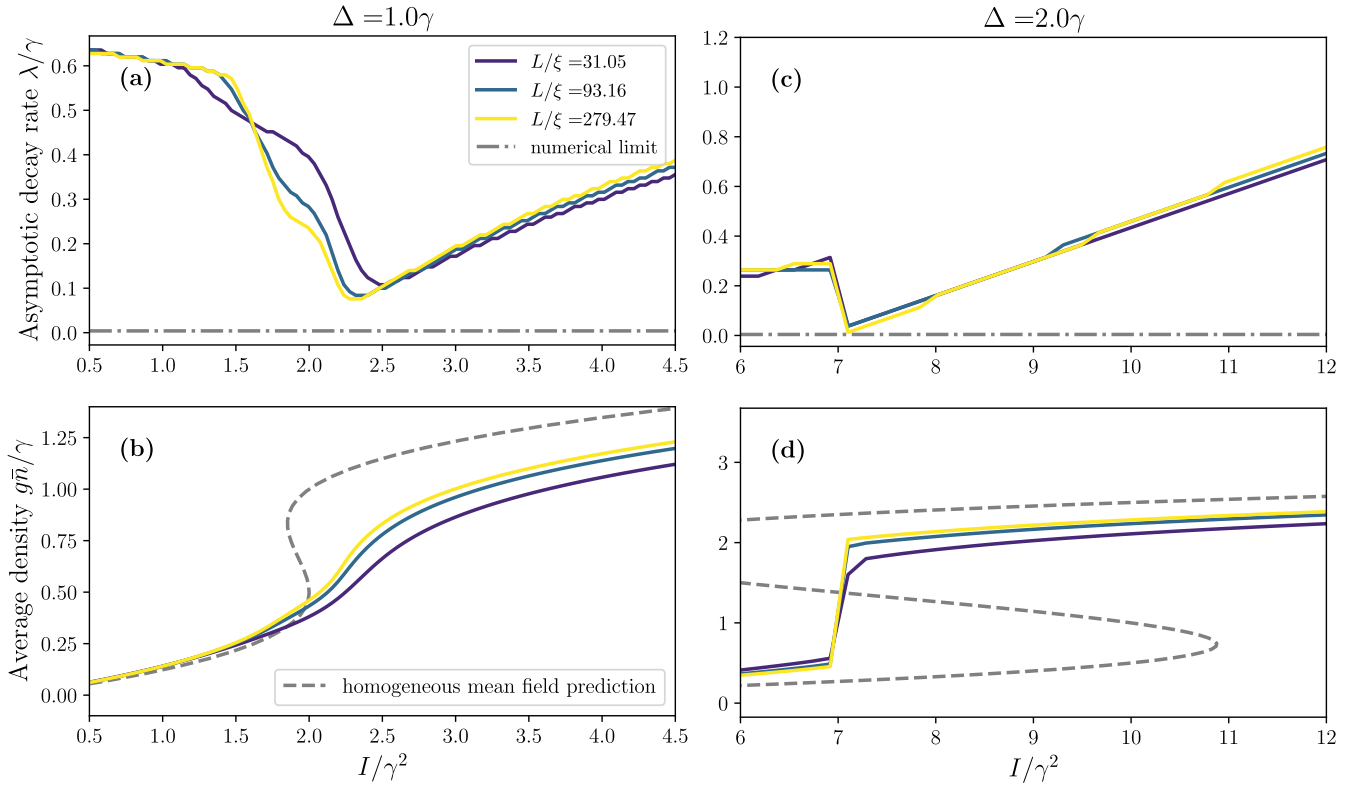


FIG. S.1. Response of the system to a Sierpinski carpet drive with fractal dimension $d_H = 1.84$. (a) Asymptotic decay rate as a function of input intensity for detuning $\Delta = \gamma$, showing no phase transition. (b) Corresponding bosonic density as a function of input intensity, with a smooth increase. (c) For a larger detuning $\Delta = 2.0\gamma$, the minimal asymptotic decay rate λ_{\min} vanishes at the critical point $I_c \approx 7.1\gamma^2$, indicating a first-order phase transition. (d) At the same critical point, the average bosonic density exhibits a discontinuous jump.

THE SPATIAL PROFILES OF THE STUDIED FRACTALS

Figure S.2 shows the spatial profiles of the patterns analyzed in the main text (Fig. 3). In addition to the standard 2D and 1D reference patterns, we include several variations of the Sierpinski cross and carpet, as well as modified versions of the Cantor set with fractal dimension lower than one. One particular geometry (the last one on the left in Fig. S.2) is not shown in the main text, as the asymptotic decay rate did not converge in the thermodynamic limit within the range of system sizes we were able to simulate.

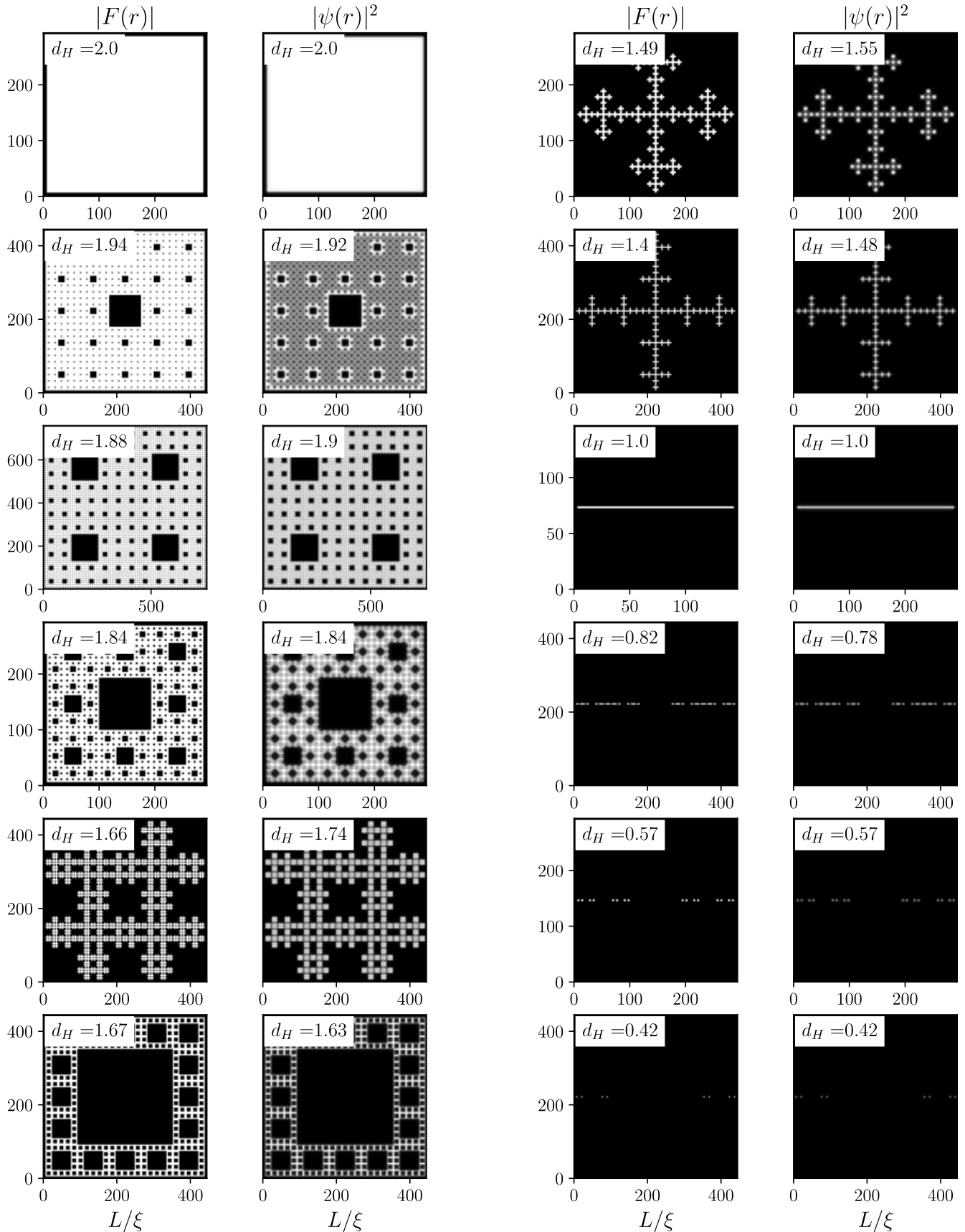


FIG. S.2. Left panels: 2D square geometry ($d_H = 2$) and several variations of the Sierpinski carpet with fractal dimensions in the range $1 < d_H < 2$. Right panels: Variations of the Sierpinski cross ($1 < d_H < 2$) in the first two rows, followed by the 1D strip ($d_H = 1$) in the third row. The final row shows variations of the Cantor set with $d_H < 1$. All patterns are computed with $\Delta = \gamma$, and the driving amplitudes are tuned to their respective critical points. The geometries and system sizes correspond to those used in Fig. 3, except for the last geometry on the left, which is excluded from the main text due to lack of convergence in the asymptotic decay rate for the considered spatial sizes.

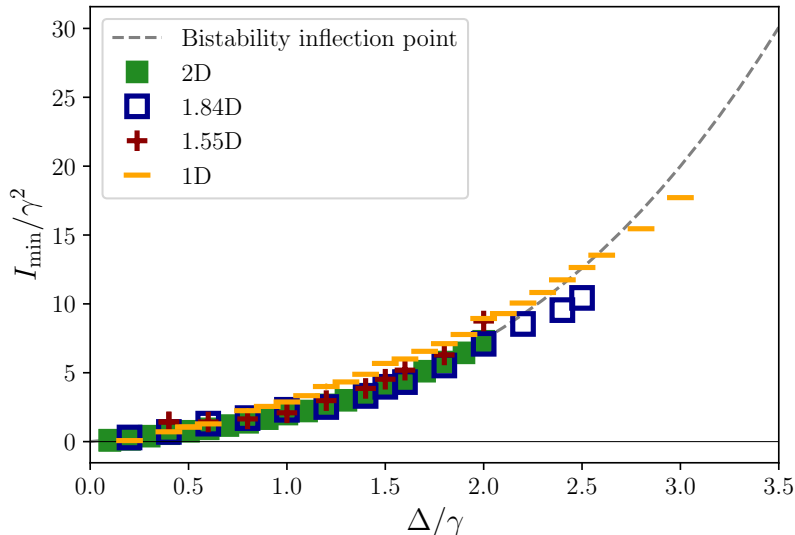


FIG. S.3. Evolution of the critical point I_{\min} as a function of Δ . A quadratic dependence is observed, consistent with estimates based on the single-mode mean-field description of the bistability curve. The inflection point of the mean-field curve (grey line) closely approximates the critical point across all geometries considered.

DEPENDENCE OF THE CRITICAL DRIVING ON THE DETUNING

In Fig. S.3, we extract the value of the driving intensity I_{\min} such that $\lambda(I_{\min}) = \lambda_{\min}$, for a range of detuning values. As a reminder, $\lambda(I)$ denotes the asymptotic decay rate of the observed pattern as a function of the driving intensity I , and λ_{\min} is its minimum value. As discussed in the main text, this minimum signals the presence of critical behavior in the system. Plotting I_{\min} as a function of detuning thus allows us to trace how the onset of criticality evolves under varying external conditions.

Interestingly, the value of I_{\min} closely matches the inflection point of the bistability curve derived from single-mode ($k = 0$) mean-field solution for the homogeneous driving case. The inflection point corresponds to the value of the driving intensity at which the curvature of the response function changes sign—specifically, where the second derivative of the driving intensity with respect to the density $n = |\psi|^2$ vanishes:

$$\frac{d^2 I}{dn^2} = 0. \quad (\text{S.1})$$

This yields the prediction

$$I_{\min} = \frac{2\Delta}{3g} \left(\frac{\Delta^2}{9} + \frac{\gamma^2}{4} \right),$$

which is shown as the grey dashed line in Fig. S.3. The close agreement between the numerical values of I_{\min} and the analytical inflection point provides a consistency check and further supports the interpretation of λ_{\min} as a reliable marker of criticality.

ASYMPTOTIC DECAY RATE AND BOGOLIUBOV INSTABILITIES

For a homogeneous driving, we can diagonalize the problem for fluctuations on top of the steady state and obtain a spectrum of the so-called dissipative Bogoliubov modes [4]. By analyzing the dispersion relation given in equation (S.2), we can interpret the phase transition as the emergence of an unstable mode.

$$\omega_{\text{Bog}}(\mathbf{k}) = \pm \left[\left(-\Delta + \frac{\hbar \mathbf{k}^2}{2m} + 2gn \right)^2 - (gn)^2 \right]^{1/2} - i\frac{\gamma}{2} \quad (\text{S.2})$$

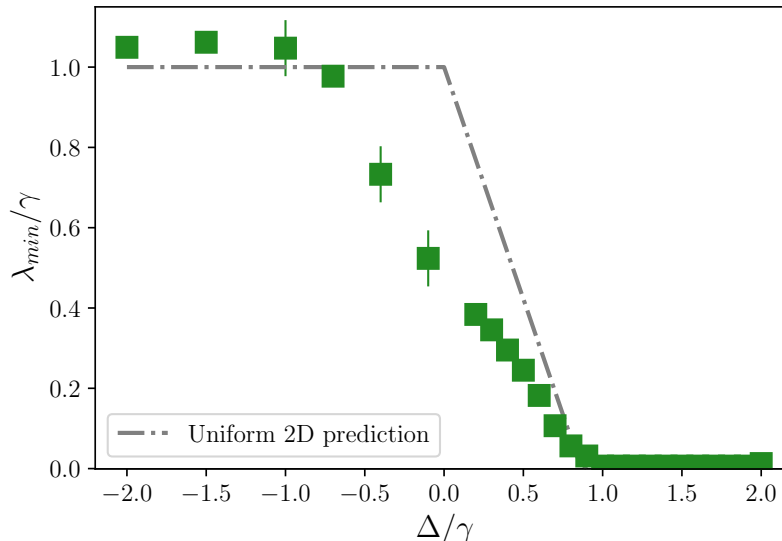


FIG. S.4. Minimal asymptotic decay rate for the 2D square geometry (green squares), computed for a system size $L = 81l$. Vertical error bars indicate the difference in λ_{\min} between this size and a smaller system with $L = 27l$. The grey dash-dotted line shows the linewidth λ_{Bog} predicted by Bogoliubov analysis for a uniform 2D system. The two curves exhibit similar behavior, with discrepancies attributed to finite-size effects.

All modes decay with the natural polariton decay rate γ ; however, this rate can be reduced and is determined by the imaginary part of ω_{Bog} . If $\text{Im}(\omega_{\text{Bog}}(\mathbf{k})) < 0$, the mode is stable and has a linewidth given by $2 \text{Im}(\omega_{\text{Bog}}(\mathbf{k}))$. The factor of 2 arises because we are considering the evolution of the bosonic density, $n(t) = |\psi(t)|^2$.

An unstable mode corresponds to $\text{Im}(\omega_{\text{Bog}}(\mathbf{k})) \geq 0$. In this case, the linewidth vanishes, the asymptotic decay rate tends to zero, and we can interpret the system as undergoing critical behavior.

We can define the minimal linewidth λ_{Bog} associated with the temporal evolution of the density of a homogeneous phase with steady-state density n_{ss} as:

$$\lambda_{\text{Bog}} = \begin{cases} 2 |\max_{k, n_{ss}} \text{Im}(\omega_{\text{Bog}}(k, n_{ss}))| & \text{if stable} \\ 0 & \text{else} . \end{cases} \quad (\text{S.3})$$

This leads to the following expression:

$$\lambda_{\text{Bog}} = \begin{cases} \gamma & \text{if } \Delta < 0 \\ \gamma - \frac{2}{\sqrt{3}}\Delta & \text{if } 0 < \Delta < \frac{\sqrt{3}}{2}\gamma \\ 0 & \text{else} . \end{cases} \quad (\text{S.4})$$

This dependence is shown as the dotted line in Fig. S.4, alongside numerical results for the 2D square geometry. Both the analytical predictions and the numerical data display a step-like behavior with a linear slope between the upper and lower values. The two curves coincide for $\Delta \gtrsim 1.0\gamma$, where the system becomes critical and $\lambda_{\min} = 0$. Deviations at other detuning values can be primarily attributed to finite-size effects.

TIME EVOLUTION OF THE DENSITY PROFILE

Additional insight can be gained by examining the time evolution of the density profile. In particular, we focus on the spatial structure of the slowest decaying mode in the fractal geometry corresponding to the Sierpinski carpet ($d_H \approx 1.8$). Figure S.5 displays the spatial dependence of the density deviation from the steady state at different time steps; specifically, we plot $|n_{ss}(\mathbf{r}) - n(\mathbf{r}, t)|$ for various times t . This local information can be compared with the global behavior shown in the upper panel of Fig. S.5, where the evolution of the spatially averaged density $\bar{n}(t)$ is presented for the same system.

At early times, the density $n(\mathbf{r}, t)$ is close to zero throughout the system, so the difference shown in the first lower panel of Fig. S.5 primarily reflects the shape of the final steady state. At later times, as shown in the final panels,

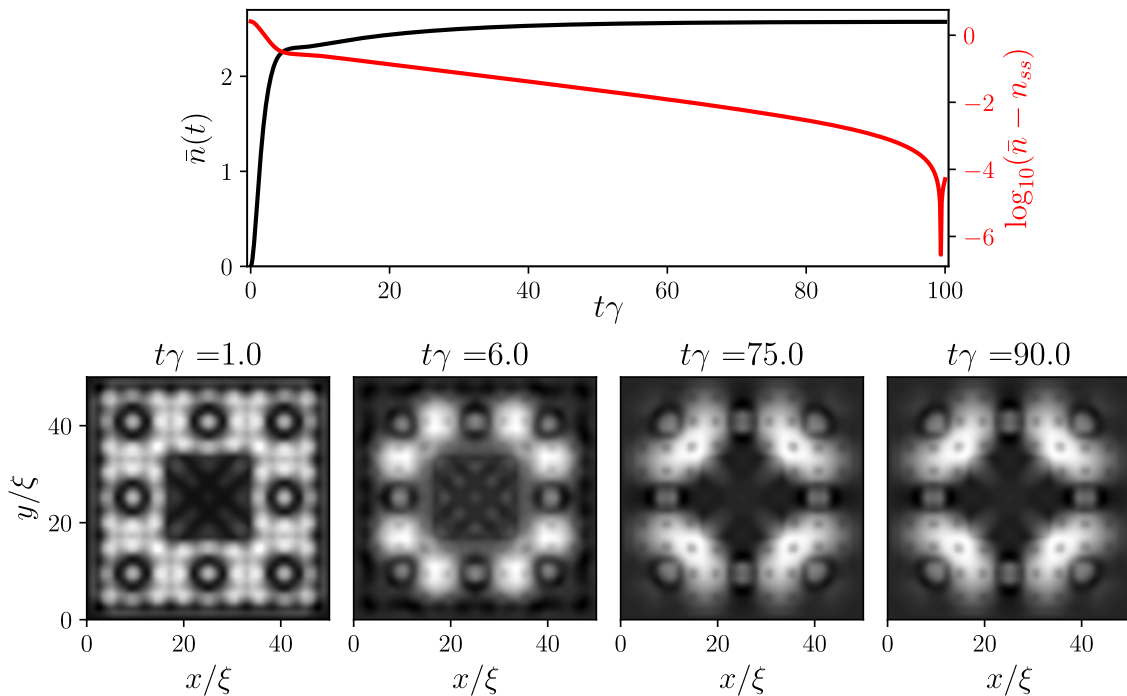


FIG. S.5. Lower panels: Spatial profile of the density deviation from the steady state at different time steps t , given by $|n_{ss}(\mathbf{r}) - n(\mathbf{r}, t)|$, for the Sierpinski carpet at the crossover point $I = 2.3\gamma^2$ with $\Delta = \gamma$. Upper panel: Time evolution of the spatially averaged density $\bar{n}(t) = \int d^2x n(t, x)$. In red, we plot the logarithm of the deviation from the steady state, making the asymptotic decay rate clearly visible.

a distinct pattern begins to emerge. This structure corresponds to the longest-lived mode—i.e., the one governing the asymptotic decay rate. In the Liouvillian framework, this is the eigenstate of the Lindbladian superoperator associated with the Liouvillian gap (the smallest nonzero eigenvalue). Thus, we are observing the mode that is key to characterizing the system's critical behavior.

For a homogeneous condensate, this connects to the dispersion relation $\omega(\mathbf{k})$ given in Eq. (S.2). In certain cases, the slowest-decaying mode (i.e., the one with the largest imaginary part of ω) occurs at a nonzero wavevector $\mathbf{k} \neq \mathbf{0}$, meaning that the longest-lived mode may not share the spatial symmetry of the driving field. In our case, the resulting mode exhibits a distinctive and nontrivial spatial structure, which will be the subject of future investigation.

CRITICAL DETUNING INDEPENDENCE FROM THE INTERACTION STRENGTH WITHIN THE NON-EQUILIBRIUM GROSS-PITAEVSKII FRAMEWORK

Within the mean-field treatment employed in this work, changing the nonlinear interaction constant g does not alter the underlying physics. In other words, when analyzing the Gross-Pitaevskii equation (1), varying g does not affect the qualitative or quantitative results.

To illustrate this, consider two systems with nonlinear interaction strengths g_1 and g_2 , and assume identical detuning and dissipation parameters: $\Delta_1 = \Delta_2 = \Delta$ and $\gamma_1 = \gamma_2 = \gamma$. Let us express $g_2 = g_1/\eta^2$, where η is a real scaling factor. The dynamics of system 2 is then governed by:

$$i \frac{d\psi_2}{dt} = \left[-\Delta - \frac{\hbar \nabla^2}{2m} + \frac{g_1}{\eta^2} |\psi_2|^2 - i \frac{\gamma}{2} \right] \psi_2 + i F_2(\mathbf{r}). \quad (\text{S.5})$$

If we rescale the driving field and wavefunction as $F_2 = \eta F_1$ and $\psi_2 = \eta \psi_1$, the equation for ψ_2 becomes identical to that of system 1. This rescaling is permissible because both F and ψ are degrees of freedom of the system and, in practice, are often expressed in arbitrary units in experimental setups.

Therefore, as long as the mean-field approximation holds, our results are invariant under changes in the absolute

value of g . However, this invariance is not expected to persist in the strongly interacting regime, which lies beyond the scope of the present work and will be explored in future studies.